Biological Charge Resonance

DOI: 10.1002/anie.201410247

Probing Bis-Fe^{IV} MauG: Experimental Evidence for the Long-Range Charge-Resonance Model**

*Jiafeng Geng, Ian Davis, and Aimin Liu**

Abstract: *The biosynthesis of tryptophan tryptophylquinone, a protein-derived cofactor, involves a long-range reaction mediated by a bis-Fe^{IV} intermediate of a diheme enzyme, MauG. Recently, a unique charge-resonance (CR) phenomenon was discovered in this intermediate, and a biological, long-distance CR model was proposed. This model suggests that the chemical nature of the bis-Fe^{IV} species is not as simple as it appears; rather, it is composed of a collection of resonance structures in a dynamic equilibrium. Here, we experimentally evaluated the proposed CR model by introducing small molecules to, and measuring the temperature dependence of, bis-Fe^{IV} MauG. Spectroscopic evidence was presented to demonstrate that the selected compounds increase the decay rate of the bis-Fe^{IV} species by disrupting the equilibrium of the resonance structures that constitutes the proposed CR model. The results support this new CR model and bring a fresh concept to the classical CR theory.*

Since its first documentation by Brocklehurst and Badgers in 1968,[1] charge-resonance (CR) phenomena have been actively researched by organic chemists.[2] In a typical CR event, one-electron oxidation of an aromatic compound generates a cation radical which spontaneously associates with its neutral parent molecule or another molecule of the cation radical to form noncovalent "sandwich-like" dimeric complexes. The former scenario stabilizes an odd number of spin/charge in a mixed-valence species, $(\Pi)_2^{\bullet+}$, and is classified as type I CR; the latter one stabilizes an even number of spin/charge in a dication diradical, $(\Pi^{\bullet+})_2$, and is classified as type II CR.[3] Notably, unique electronic absorption bands in the near-infrared (NIR) region arise from resonance stabilization of spin/charge in the CR complexes and are thereby termed as CR bands (see Figure S1 for an MO diagram).[4–7] CR complexes represent the simplest intermolecular units that carry delocalized spin/charge. Investigation of these phenomena may provide the chemical basis for electron transfer (ET), conductivity, and ferromagnetism in many organic materials and metalloporphyrin complexes.

Like many classical chemical models adopted by nature, the utilization of CR in biological systems to transiently stabilize spin/charge was first suggested in a pair of chlorophyll molecules, known as the "special pair", in bacterial photosynthetic reaction centers.[8,9] Recently, a second example was revealed from a diheme enzyme, MauG.[3] MauG is the terminal enzyme in the biogenesis pathway of a protein-derived cofactor, tryptophan tryptophylquinone (TTQ),[10] which is the catalytic center of methylamine dehydrogenase (MADH).[11] MauG possesses two *c*-type hemes in distinct spin states: one is pentacoordinate, high-spin with an axial histidine ligand and the other is hexacoordinate, low-spin with an axial histidine-tyrosine ligand set (denoted as Heme$_{5C}$ and Heme$_{6C}$, respectively, as shown in Figure 1).[10,12] The substrate of MauG is a precursor protein of MADH, preMADH.[13] MauG performs three cycles of H_2O_2-dependent oxidation on two adjacent tryptophan residues of preMADH to produce TTQ (Figure S2a).[14] Each two-electron oxidation cycle is suggested to be mediated by a unique bis-Fe^{IV} intermediate of MauG in which Heme$_{5C}$ is in an oxyferryl state and Heme$_{6C}$ is in a ferryl state with its two original axial ligands retained (Figure S2b).[15,16]

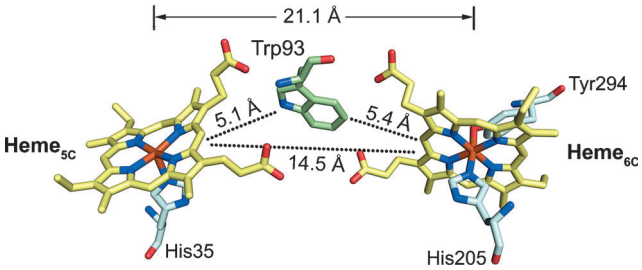

Figure 1. Structural orientation of the hemes and the intervening tryptophan residue in MauG (PDB entry: 3L4M). The distance between the two iron ions and the edge-to-edge distances between the aromatic moieties are labeled.

It is in the bis-Fe^{IV} intermediate that the CR phenomenon was proposed.[3] A broad electronic absorption band centered at 950 nm (ε = ca. 7000 $M^{-1}cm^{-1}$) is present specifically in the bis-Fe^{IV} state of MauG (Figure S2c).[3] It is noteworthy that the spectral properties of the NIR band are highly reminiscent of the reported CR spectroscopic signatures from metalloporphyrin complexes.[7,17] The bis-Fe^{IV} species is electronically equivalent to two ferric hemes each coupled with

[*] Dr. J. Geng, I. Davis, Prof. Dr. A. Liu
Department of Chemistry and Center for Diagnostics & Therapeutics, Georgia State University
Atlanta, GA (USA)
E-mail: Feradical@gsu.edu
Homepage: http://Feradical.gsu.edu

[**] We thank Dr. Victor Davidson for providing us with the expression system of MauG. This work was supported by the National Institutes of Health (grant R01GM108988) and the Georgia Research Alliance Distinguished Scholar Program (A.L.). J.G. acknowledges the William M. Suttles doctoral research fellowship and the doctoral dissertation grant from Georgia State University, and I.D. acknowledges the Molecular Basis of Disease graduate fellowship at Georgia State University.

Supporting information for this article is available on the WWW under http://dx.doi.org/10.1002/anie.201410247.

a porphyrin cation radical, a scenario resembling the dication diradical complexes in type II CR. However, this case cannot be simply illustrated by the classical CR models as the two porphyrin rings are about 14 Å apart (Figure 1), a much wider separation than the interacting moieties in model CR complexes.[18,19] A significant conformational change that enables the diheme cofactor to fold into a "sandwich-like" dimer is unlikely to occur during the formation of the bis-Fe^{IV} species since the structure shown in Figure 1 was previously demonstrated to be in the catalytically active form by reactions in crystals.[12] Thus, a new class of CR, type III, was proposed, whereby resonance stabilization of spin/charge is facilitated by an additional π moiety, the Trp93 residue located between the hemes (Figure 2a).[3] Electron/hole hopping through Trp93 was postulated to occur in the ET process between the hemes to enable CR stabilization. Ultrafast and reversible ET with Trp93 as the hopping site mimics the distribution of spin/charge as if this was in an extended conjugated system. Overall, the type III CR model represents a dynamic equilibrium of different electronically equivalent resonance structures as one electron from Trp93 cannot simultaneously fill two holes. This new CR model is supported by theoretical calculations, which predicted that in the bis-Fe^{IV} species electron/hole hopping through Trp93 makes possible a rate of interheme ET greater than $10^7\ s^{-1}$, in accordance with the reported ET rates from established model CR systems.[3]

In this work, we aim to experimentally evaluate the proposed type III CR model and determine the chemical nature of bis-Fe^{IV} MauG, i.e., whether it is a single redox species or composed of multiple resonance structures as predicted by the CR model. We introduced small-molecule ligands to disrupt the hypothesized equilibrium of high-valence species. The selected ligand molecules include cyanide (CN^-), imidazole (IM), and fluoride (F^-). They are all capable of binding to the heme iron when there is a coordinate vacancy, yet with different binding affinities. If bis-Fe^{IV} MauG is a single redox species, exogenous small-molecule ligands (CN^-, for instance) are not expected to cause a notable effect on its chemical properties because both hemes are coordinatively saturated and the axial ligands are either irreplaceable ($Heme_{5C}$) or inaccessible ($Heme_{6C}$).[12,20] However, if bis-Fe^{IV} MauG represents an equilibrium of resonance structures as proposed in Figure 2a, exogenous CN^- might be able to specifically target species like compound (Cpd) ES* and Cpd I* by outcompeting the relatively weakly associated axial ligand of $Heme_{5C}$ to generate the [$Fe^{III}CN^-\cdots Trp93^{\bullet+}\cdots Fe^{IV}$] and [$Fe^{III}CN^-\cdots Trp93\cdots Fe^{IV\bullet+}$] complexes, respectively (Figure 2b). Neither CN^- adduct is likely to be capable of maintaining the CR stabilization due to changes in heme redox properties, and it is anticipated that they will quickly decay to a stable, reduced state by releasing two oxidizing equivalents to the protein matrix or the solvent (Figure 2b). Previously, three methionine residues near $Heme_{5C}$ were identified to absorb the oxidizing equivalents from bis-Fe^{IV} in the absence of preMADH through ancillary ET pathways.[21] Despite the fact that Cpd ES* and Cpd I* are present only as minor species in the proposed CR model,[3] the dynamic exchange with other resonance structures allows the CN^--induced disruption to gradually shift the equilibrium and break the electronic communication between the hemes. It will eventually destroy the CR stabilization, resulting in an accelerated decay of the bis-Fe^{IV} species to a diferric CN^- adduct (Figure 2b).

In the absence of preMADH, bis-Fe^{IV} MauG does not misfire but instead exhibits extraordinary stability with a half-life of several minutes.[15,22] The NIR band at 950 nm can be used as a spectral signature to monitor the decay process of the bis-Fe^{IV} species.[3] Figure 3a shows that the introduction of CN^- to the bis-Fe^{IV} species led to an apparent increase in the decay rate of the NIR band, compared to a parallel experiment without CN^-. In the presence of 25 mM CN^-, the NIR spectral signature became completely diminished ca. 75 s after addition of CN^-, with a decay rate nearly one order of magnitude greater than that in the absence of CN^-. When different small-molecule ligands were examined, they exhibited different degrees of disruptive effects on the decay rate of

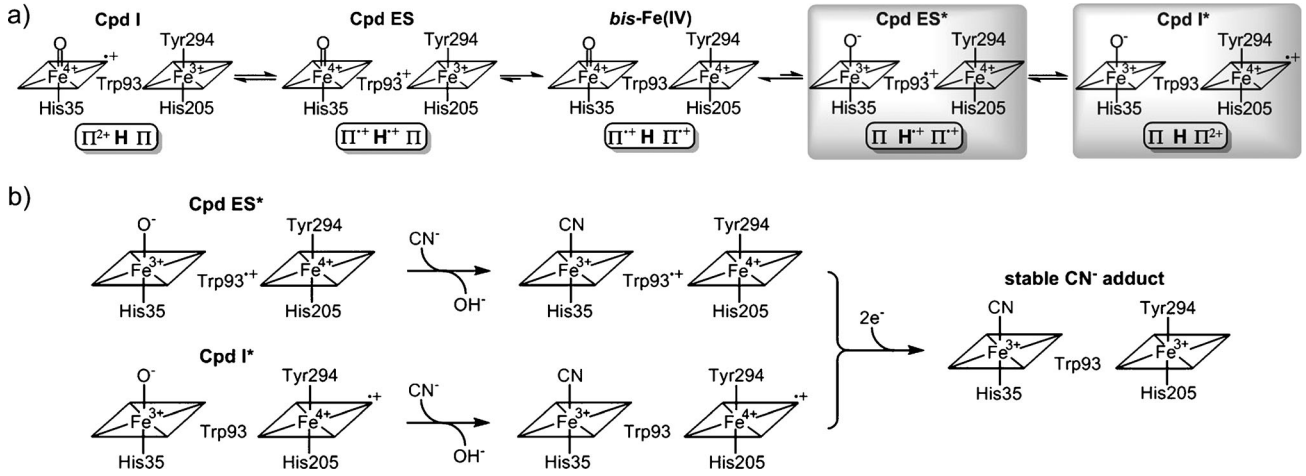

Figure 2. Type III CR in bis-Fe^{IV} MauG. a) Proposed resonance structures in the type III CR model. "H" represents a third aromatic moiety (i.e., the Trp93 residue in this case), which functions as a hopping relay to facilitate ET between the two primary aromatic moieties. The two resonance structures (Cpd ES* and Cpd I*) that can be potentially targeted by small-molecule ligands are highlighted with a grey background. b) Specific targeting of Cpd ES* and Cpd I* by CN^- to disrupt the type III CR in the bis-Fe^{IV} species.

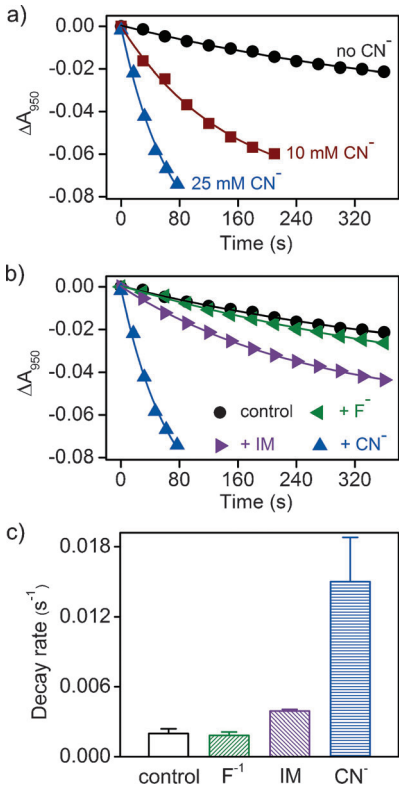

Figure 3. Disruption of bis-Fe^{IV} MauG by small-molecule ligands. a) Addition of CN^- accelerated the decay of the NIR band of bis-Fe^{IV} MauG. CN^- was added immediately after bis-Fe^{IV} formation. The solid lines are fits of the data to single-exponential decay. b) Effect of different small-molecule ligands on the decay of the NIR band. Each small-molecule ligand (25 mM) was added immediately after bis-Fe^{IV} formation. c) Decay rates of the NIR band in the absence and presence of small-molecule ligands.

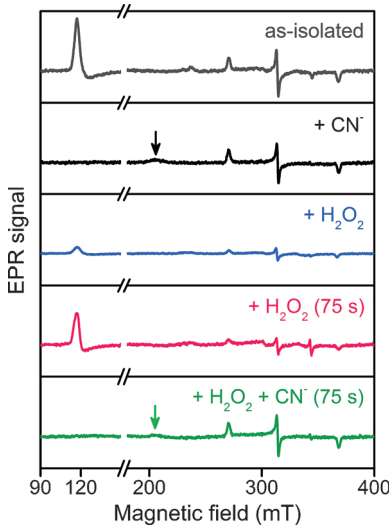

Figure 4. EPR spectra of MauG. Gray trace: as-isolated diferric MauG; black trace: MauG + 25 mM CN^-; blue trace: MauG + 1 × H_2O_2; red trace: MauG + 1 × H_2O_2 (frozen 75 s after reaction); green trace: MauG + 1 × H_2O_2 + 25 mM CN^- (CN^- was added immediately after addition of H_2O_2 and the sample was frozen 75 s after addition of CN^-). The arrows indicate the CN^- adduct of $Heme_{5C}$ at $g = 3.37$.

the NIR band with CN^- presenting the most pronounced influence, followed by IM (Figure 3b). The F^- anion showed almost no observable effect. This trend correlates with the binding affinities of these small-molecule ligands to ferric heme centers; it is known that in many hemoproteins diatomic molecules like CN^- are the most tightly associated ligands, whereas small heterocyclic compounds like IM and halide anions are usually weaker ligands.[23,24] Figure 3c summarizes the decay rates of the NIR band in the absence and presence of these small-molecule ligands.

EPR spectroscopy was also used to characterize the aforementioned chemical events. As shown in the gray trace of Figure 4, there are three different heme species revealed from the EPR spectrum of diferric MauG, a high-spin species ($Heme_{5C}$), a major low-spin species ($Heme_{6C}$), and a minor low-spin species attributed as a freezing-induced artifact derived from the high-spin species.[10,25,26] Exogenous CN^- was only able to coordinate to $Heme_{5C}$ and caused a spin transition to produce a new low-spin species with a very broad signal around $g = 3.37$, at the expense of the high-spin species (Figure 4, the black trace). This low-spin signal is consistent with the formation of a hexacoordinate CN^- adduct of $Heme_{5C}$, based on its similarity to the EPR signals of CN^- adducts reported from other hemoproteins.[27] In addition, the freezing-induced artifact was removed in the presence of CN^-, confirming that it is derived from the high-spin species of $Heme_{5C}$. Upon addition of H_2O_2 to diferric MauG, the high-spin and low-spin ferric signals are nearly absent, owing to the formation of the bis-Fe^{IV} species (Figure 4, the blue trace).[15] The introduction of CN^- to this system accelerated the decay of the newly generated bis-Fe^{IV} species as indicated by a more rapid return of the low-spin signal of $Heme_{6C}$, compared to a control sample without CN^- (Figure 4, the red and green traces). It should be noted that $Heme_{6C}$ is buried in the protein matrix and inaccessible to exogenous small-molecule ligands.[12,20] Thus, the accelerated decay of the ferryl species at the $Heme_{6C}$ site is likely due to disruptive events that remotely occurred at the $Heme_{5C}$ site and caused a loss of the electronic communication between the two hemes. The sample freeze-quenched 75 s after addition of CN^- to bis-Fe^{IV} MauG displayed a spectrum that is almost identical to that of the sample containing the CN^- adduct of MauG (Figure 4, the black and green traces). This observation suggests that almost all the newly generated bis-Fe^{IV} species was eliminated after the CN^- treatment for 75 s, consistent with the result obtained from monitoring the decay of the NIR band. It also indicates that the end product of this chemical processing is a diferric CN^- adduct of MauG, in accordance with our proposed scheme shown in Figure 2b.

Given the relatively high concentration of small-molecule ligands added to the system, it could be possible that direct reduction by these molecules or exchange of the ferryl oxo group with exogenous ligands occurred at the $Heme_{5C}$ site, thereby causing a more rapid decay of bis-Fe^{IV} MauG. Our further investigation on the Y294H mutant of MauG ruled out this possibility. Tyr294 is an axial ligand of $Heme_{6C}$ (Figure 1). Mutation of this residue to histidine creates an axial bis-histidine ligand set at $Heme_{6C}$, which is not capable

of stabilizing the ferryl oxidation state.[28] In the reaction between diferric Y294H MauG and H_2O_2, the two oxidizing equivalents from H_2O_2 are trapped at the $Heme_{5C}$ site in the form of a Cpd I-like species (Figure S3a), which presents a characteristic absorption band for Cpd I species at 655 nm but no NIR band at 950 nm (Figure S3b).[28,29] The introduction of small-molecule ligands such as CN^- and IM to Y294H Cpd I had a minimal effect on its decay rate as revealed from the time-dependent spectral change at 655 nm (Figure S3c). Therefore, the observed accelerated decay of the bis-Fe^{IV} species from wild-type MauG in the presence of small-molecule ligands is unlikely due to direct reduction or ligand exchange on the oxyferryl species at the $Heme_{5C}$ site.

Furthermore, the effect of temperature on the spectral and kinetic properties of the NIR absorption feature was investigated over a temperature range of 2 to 30 °C. As reported from a previous study, MauG is not stable above the higher temperature,[30] thereby limiting the temperature range. Within this interval, changes in temperature have no observable effect on the absorption maxima wavelength or the overall lineshape of the NIR band; however, the absorption intensity was seen to increase with decreasing temperature. Figure 5 shows that the decay rate of the NIR

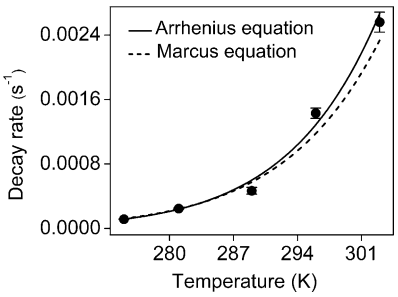

Figure 5. Temperature effect on the decay rate of the NIR band of bis-Fe^{IV} MauG. The bis-Fe^{IV} species was generated by addition of a stoichiometric amount of H_2O_2 to diferric MauG (15 μM). The data were fit to the Arrhenius equation (solid trace) to calculate the activation energy (E_a) and to the Marcus equation (dashed line) to calculate the reorganization energy (λ) of the ET reaction, respectively.

band increases as the temperature rises. Fitting of the experimental data by the Arrhenius equation [Eq. (S1)] yields an activation energy (E_a) of 18.6 kcal mol^{-1}. As mentioned previously, the decay of the NIR band is associated with the decay of the bis-Fe^{IV} species through oxidation of the methionine residues near $Heme_{5C}$. The E_a value of the bis-Fe^{IV} self-decay reaction is comparable but slightly higher than those determined from H_2O_2-dependent oxidation reactions of methionine residues in other proteins or peptides.[31,32] The self-decay process of the bis-Fe^{IV} species can be also treated as an ET reaction from the methionine residues to the diheme cofactor. The experimental data was also analyzed using the classical ET theory[33] (see details in the Supporting Information). Among the three methionine residues near $Heme_{5C}$, Met108 was identified as the first residue to be oxidized by bis-Fe^{IV} MauG.[21] The ET reaction was analyzed with Met108 as the electron donor and the diheme cofactor as the electron acceptor. Using the direct distance approach developed by Dutton and co-workers,[34] a HARLEM[35] calculation on this ET reaction revealed an ET distance (r) of 7.31 Å and a decay constant (β) of 1.64 Å. Although the free energy change ($\Delta G°$) of this ET reaction is unknown, it can be estimated based on the redox potentials of the associated redox centers.[36,37] The reaction potential ($E°$) is anticipated to be within the range of 0 to 1 V, corresponding to a range of 0 to −23.1 kcal mol^{-1} for $\Delta G°$. In Figure 5, fitting of the experimental data by the Marcus equation [Eq. (S2)] with the input of these calculated parameters yields a range of the reorganization energy (λ) of 3.02 to 4.81 eV. This range is comparable but slightly larger than those calculated for other ET reactions from similar systems.[30] The increased values of E_a and λ for the bis-Fe^{IV} self-decay reaction highlight the role of CR in stabilizing the bis-Fe^{IV} species by elevating the energy barrier for self-oxidation reactions. This is achieved by expanding the single redox center to an extended conjugated system and thereby increasing the reorganization energy of the related ET reactions.

In conclusion, the bis-Fe^{IV} state of MauG is not a single redox species but rather an equilibrium of different electronically equivalent resonance structures. The data presented here provide supporting evidence for our proposed long-distance type III CR model, which brings a new concept to the well-documented CR phenomena.

Received: October 20, 2014
Revised: December 14, 2014
Published online: January 29, 2015

Keywords: charge resonance · electronic structure · heme proteins · high-valence iron · near-infrared spectroscopy

[1] B. Badger, B. Brocklehurst, *Nature* **1968**, *219*, 263.
[2] A. Heckmann, C. Lambert, *Angew. Chem. Int. Ed.* **2012**, *51*, 326–392; *Angew. Chem.* **2012**, *124*, 334–404.
[3] J. Geng, K. Dornevil, V. L. Davidson, A. Liu, *Proc. Natl. Acad. Sci. USA* **2013**, *110*, 9639–9644.
[4] J. K. Kochi, R. Rathore, P. L. Magueres, *J. Org. Chem.* **2000**, *65*, 6826–6836.
[5] A. Takai, C. P. Gros, J. M. Barbe, R. Guilard, S. Fukuzumi, *Chem. Eur. J.* **2009**, *15*, 3110–3122.
[6] A. Bloch-Mechkour, T. Bally, A. Marcinek, *J. Phys. Chem. A* **2011**, *115*, 7700–7708.
[7] K. E. Brancato-Buentello, S. J. Kang, W. R. Scheidt, *J. Am. Chem. Soc.* **1997**, *119*, 2839–2846.
[8] J. Breton, E. Nabedryk, W. W. Parson, *Biochemistry* **1992**, *31*, 7503–7510.
[9] P. Kanchanawong, M. G. Dahlbom, T. P. Treynor, J. R. Reimers, N. S. Hush, S. G. Boxer, *J. Phys. Chem. B* **2006**, *110*, 18688–18702.
[10] Y. Wang, M. E. Graichen, A. Liu, A. R. Pearson, C. M. Wilmot, V. L. Davidson, *Biochemistry* **2003**, *42*, 7318–7325.
[11] W. S. McIntire, D. E. Wemmer, A. Chistoserdov, M. E. Lidstrom, *Science* **1991**, *252*, 817–824.
[12] L. M. R. Jensen, R. Sanishvili, V. L. Davidson, C. M. Wilmot, *Science* **2010**, *327*, 1392–1394.
[13] A. R. Pearson, T. De La Mora-Rey, M. E. Graichen, Y. Wang, L. H. Jones, S. Marimanikkupam, S. A. Agger, P. A. Grimsrud, V. L. Davidson, C. M. Wilmot, *Biochemistry* **2004**, *43*, 5494–5502.

[14] E. T. Yukl, F. Liu, J. Krzystek, S. Shin, L. M. R. Jensen, V. L. Davidson, C. M. Wilmot, A. Liu, *Proc. Natl. Acad. Sci. USA* **2013**, *110*, 4569 – 4573.
[15] X. Li, R. Fu, S. Lee, C. Krebs, V. L. Davidson, A. Liu, *Proc. Natl. Acad. Sci. USA* **2008**, *105*, 8597 – 8600.
[16] J. Geng, I. Davis, F. Liu, A. Liu, *J. Biol. Inorg. Chem.* **2014**, *19*, 1057 – 1067.
[17] J. H. Fuhrhop, P. Wasser, D. Riesner, D. Mauzerall, *J. Am. Chem. Soc.* **1972**, *94*, 7996 – 8001.
[18] S. V. Lindeman, S. V. Rosokha, D. Sun, J. K. Kochi, *J. Am. Chem. Soc.* **2002**, *124*, 843 – 855.
[19] H. Song, R. D. Orosz, C. A. Reed, W. R. Scheidt, *Inorg. Chem.* **1990**, *29*, 4274 – 4282.
[20] R. Fu, F. Liu, V. L. Davidson, A. Liu, *Biochemistry* **2009**, *48*, 11603 – 11605.
[21] E. T. Yukl, H. R. Williamson, L. Higgins, V. L. Davidson, C. M. Wilmot, *Biochemistry* **2013**, *52*, 9447 – 9455.
[22] S. Lee, S. Shin, X. Li, V. L. Davidson, *Biochemistry* **2009**, *48*, 2442 – 2447.
[23] F. Viola, S. Aime, M. Coletta, A. Desideri, M. Fasano, S. Paoletti, C. Tarricone, P. Ascenzi, *J. Inorg. Biochem.* **1996**, *62*, 213 – 222.
[24] W. C. Winkler, G. Gonzalez, J. B. Wittenberg, R. Hille, N. Dakappagari, A. Jacob, L. A. Gonzalez, M. A. Gilles-Gonzalez, *Chem. Biol.* **1996**, *3*, 841 – 850.
[25] Y. Chen, S. G. Naik, J. Krzystek, S. Shin, W. H. Nelson, S. Xue, J. J. Yang, V. L. Davidson, A. Liu, *Biochemistry* **2012**, *51*, 1586 – 1597.
[26] M. Feng, L. M. R. Jensen, E. T. Yukl, X. Wei, A. Liu, C. M. Wilmot, V. L. Davidson, *Biochemistry* **2012**, *51*, 1598 – 1606.
[27] S. Van Doorslaer, L. Tilleman, B. Verrept, F. Desmet, S. Maurelli, F. Trandafir, L. Moens, S. Dewilde, *Inorg. Chem.* **2012**, *51*, 8834 – 8841.
[28] N. Abu Tarboush, L. M. R. Jensen, M. Feng, H. Tachikawa, C. M. Wilmot, V. L. Davidson, *Biochemistry* **2010**, *49*, 9783 – 9791.
[29] N. Abu Tarboush, S. Shin, J. F. Geng, A. M. Liu, V. L. Davidson, *FEBS Lett.* **2012**, *586*, 4339 – 4343.
[30] M. Choi, S. Shin, V. L. Davidson, *Biochemistry* **2012**, *51*, 6942 – 6949.
[31] B. Pan, J. Abel, M. S. Ricci, D. N. Brems, D. I. Wang, B. L. Trout, *Biochemistry* **2006**, *45*, 15430 – 15443.
[32] R. Thirumangalathu, S. Krishnan, P. Bondarenko, M. Speed-Ricci, T. W. Randolph, J. F. Carpenter, D. N. Brems, *Biochemistry* **2007**, *46*, 6213 – 6224.
[33] R. A. Marcus, N. Sutin, *Biochim. Biophys. Acta Rev. Bioenerg.* **1985**, *811*, 265 – 322.
[34] C. C. Page, C. C. Moser, X. X. Chen, P. L. Dutton, *Nature* **1999**, *402*, 47 – 52.
[35] I. V. Kurnikov, HARLEM—Molecular Modeling Package **2000**, http://harlem.chem.cmu.edu/index.php.
[36] J. Bergès, P. de Oliveira, I. Fourre, C. Houee-Levin, *J. Phys. Chem. B* **2012**, *116*, 9352 – 9362.
[37] G. Battistuzzi, M. Bellei, C. A. Bortolotti, M. Sola, *Arch. Biochem. Biophys.* **2010**, *500*, 21 – 36.

